Eur. J. Mineral.
2011, **23**, 467–473
Published online March 2011

Yangzhumingite, $KMg_{2.5}Si_4O_{10}F_2$, a new mineral in the mica group from Bayan Obo, Inner Mongolia, China

RITSURO MIYAWAKI[1,*], HIDEHIKO SHIMAZAKI[1,2], MASAKO SHIGEOKA[1], KAZUMI YOKOYAMA[1], SATOSHI MATSUBARA[1] and HISAYOSHI YURIMOTO[3]

[1] Department of Geology and Paleontology, the National Museum of Nature and Science, 3-23-1, Hyakunin-cho, Shinjuku, Tokyo 169-0073, Japan
*Corresponding author, e-mail: miyawaki@kahaku.go.jp
[2] University of Tokyo, Hongo, Bunkyo, Tokyo 113-0033, Japan
[3] Department of Natural History Sciences, Hokkaido University, Sapporo 060-0810, Japan

Abstract: Yangzhumingite, ideally $KMg_{2.5}Si_4O_{10}F_2$, occurs as subhedral to euhedral platy crystals up to *ca.* 0.5 mm across in metamorphosed carbonate rock from Bayan Obo, Inner Mongolia, China. It is associated with dolomite, calcite, tremolite, norbergite and huanghoite-(Ce) with minor phlogopite, barite, bastnäsite-(Ce), parisite-(Ce), and fluorite. Yangzhumingite is transparent and colorless with white streak and pearly luster. It is optically biaxial (–), $n = 1.532$–1.537 (589 nm), and $2V = 5$–$10°$. The hardness is 3 on Mohs' scale (measured on a synthetic equivalent). It has a monoclinic unit cell with $a = 5.249(4)$, $b = 9.095(5)$, $c = 10.142(5)$ Å, $\beta = 99.96(6)°$, $V = 476.9(5)$ Å^3, $Z = 2$, space group $C2/m$, and $D_{calc.} = 2.807$ g/cm^3. The five strongest lines in the powder XRD pattern are [d(Å), I/I_0, hkl]: (10.03, 95, 001); (3.37, 48, 022), (2.90, 49, 11$\bar{3}$), (2.59, 67, 13$\bar{1}$ 200) and (2.41, 100, 13$\bar{2}$ 201). The mean of 15 electron microprobe analyses and SIMS analysis for Li lead to the empirical formula $(K_{0.70}Li_{0.30}Na_{0.01})(Mg_{2.48}Fe_{0.06})(Si_{3.96}Al_{0.03})O_{10}[F_{1.92}(OH)_{0.08}]$ on the basis of 12 anions with (F + OH) = 2. Yangzhumingite is a member of the mica group (Nickel-Strunz grouping 9.EC.10), and it represents the Mg-dominant analogue of montdorite.

Key-words: yangzhumingite, new mineral, Bayan Obo, mica group, tetrasilicic, lithium, fluorine.

1. Introduction

Micaceous grains were recognized in a thin section of a specimen of metamorphosed carbonate rock from Bayan Obo, Inner Mongolia, China. The metamorphosed carbonate rock was collected from the outcrop same to that of the deep purple fluorite rock including the type specimen of zhangpeishanite, BaFCl (Shimazaki *et al.*, 2008a). The studied material has been reported by Shimazaki *et al.* (2008b) as the mica showing a characteristic chemistry, Al- and Fe-free. The mineral and name were approved by the IMA Commission on New Minerals, Nomenclature and Classification (IMA2009-017). The name is for Prof. Yang, Zhuming (born 1951), mineralogist and crystallographer, in recognition of his contributions to the mineralogy of Bayan Obo. The type material is housed in the National Museum of Nature and Science, Tokyo, Japan and the Institute of Geology and Geophysics, Chinese Academy of Sciences, Beijing, China under the registered number NSM-MF15361 and KDX015, respectively.

2. Geological background and occurrence

Bayan Obo, a world-class Nb–REE–Fe deposit, is located in Inner Mongolia, China (109°57′E, 41°46′N). The deposit extends approximately 36 km in the east–west direction and has a variable width between 0.5 and 5 km. The East and Main orebodies are the two major Nb–REE–Fe orebodies among several other smaller ones. Nearly 200 mineral species have been so far identified from the Bayan Obo deposit (*e.g.*, Zhang & Tao, 1986).

Yangzhumingite occurs in one of the band textures of metamorphosed carbonate rock found in the transition zone between the dolomite and slate at the southern part of East orebody, Bayan Obo. Associated minerals in the Al- and Fe-deficient part are: dolomite, calcite, tremolite, norbergite and huanghoite-(Ce) with minor phlogopite, barite, bastnäsite-(Ce), parisite-(Ce) and fluorite. The metamorphosed carbonate rock consists of calcite and dolomite, with minor fluorite, barite, fluorapatite, bastnäsite-(Ce), cordylite-(Ce), monazite-(Ce), zircon, thorianite, norsethite, magnetite, hematite, goethite,

DOI: 10.1127/0935-1221/2011/0023-2098
0935-1221/11/0023-2098 $ 3.15

pyrite, pyrrhotite and galena. Fluorotetraferriphlogopite (Miyawaki *et al.*, 2011) was recognized in another band with some Fe-bearing minerals such as norbergite, richterite and serpentine. Although the origin of yangzhumingite can not be specified owing to the complex geological setting, the mineral may have formed during a stage of hydrothermal activity or later metamorphic activity.

3. Appearance and physical and optical properties

Yangzhumingite occurs as subhedral to euhedral platy crystals ranging in size from several tens to several hundreds of micrometers across (Fig. 1). It is transparent and colorless with white streak and pearly luster. No fluorescence was observed under short or long wave UV light. Hardness could not be measured because of small grain size. The synthetic equivalent (Topy Industry Limited, PDM-K(G)325 potassium tetrasilicic mica) showed 3 on the Mohs hardness scale. Yangzhumingite is flexible and elastic. It shows a perfect cleavage on {001}. Density of yangzhumingite could not be measured because of small grain size, whereas the calculated density is 2.807 g/cm^3 on the basis of the empirical formula and unit-cell values. The optical data of yangzhumingite are: biaxial (–), n(minimum) = 1.532, n(maximum) = 1.537 (589 nm), and $2V$ (meas.) = 5–10°. No pleochroism was observed.

4. Chemical composition

Chemical analyses of yangzhumingite (15 spots) were carried out by means of an electron microprobe JEOL JXA-8800M, operating at 15 kV and 20 nA, with 2 μm beam diameter. The Li content was determined by means of a Cameca IMS-3f secondary ion mass spectrometer (SIMS) at Hokkaido University. The primary ion beam was mass filtered $^{16}O^-$-accelerated to 14.5 keV and adjusted for a beam current of about 7 nA with a spot size of about 10 μm. Kinetic energy filtering was achieved by offsetting the sample accelerating voltage (–100 V) while keeping the setting of the electrostatic analyzer and the width and position of the energy slit constant. The energy band-pass was set to accept a 20 eV window. Positive secondary ions of $^{28}Si^+$ and $^{7}Li^+$ were measured under a mass resolving power of ~500. A zinnwaldite crystal with known Li content was used for standardization. Other analytical conditions were similar to those employed by Yurimoto *et al.* (1989). The amount of H_2O was calculated by stoichiometry using (F + OH) = 2. Analytical data are given in Table 1. The empirical formula of yangzhumingite is $(K_{0.70}Li_{0.30}Na_{0.01})(Mg_{2.48}Fe_{0.06})(Si_{3.96}Al_{0.03})O_{10}[F_{1.92}(OH)_{0.08}]$ or $(K_{0.70}Na_{0.01})(Mg_{2.48}Li_{0.30}Fe_{0.06})(Si_{3.96}Al_{0.03})O_{10}[F_{1.92}(OH)_{0.08}]$ on the basis of 12 anions and (F + OH) = 2. Regardless of the structural position of Li, as shown below, the ideal formula is $KMg_{2.5}Si_4O_{10}F_2$, which requires K_2O 11.48, MgO 24.56, SiO_2 58.59, F 9.26, F = O −3.90, total 100 wt%.

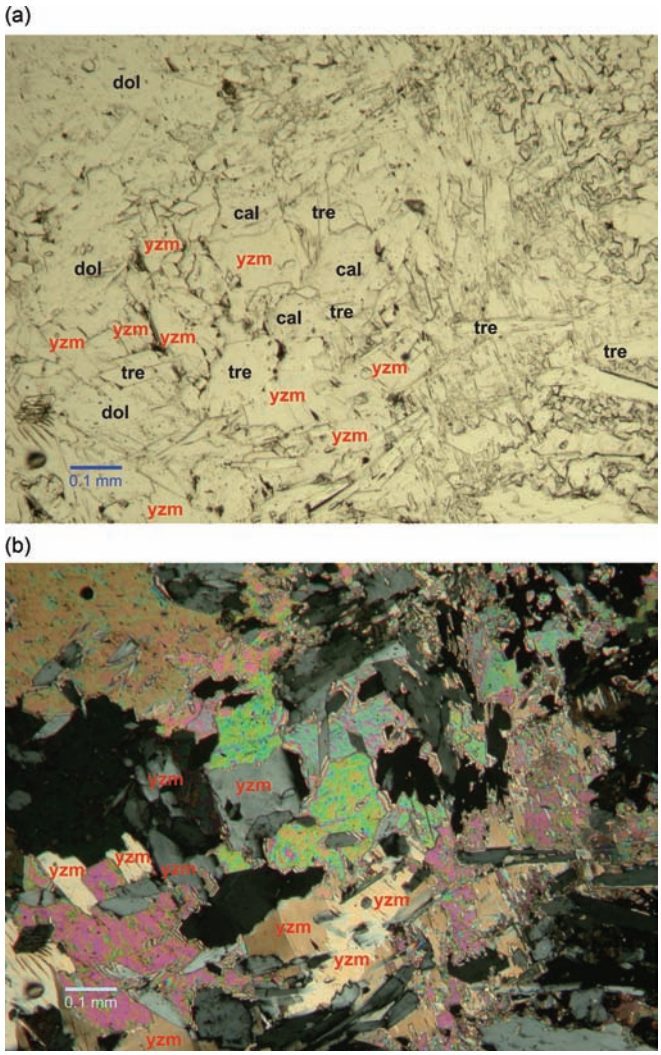

Fig. 1. Photomicrographs of yangzhumingite (yzm) in association with dolomite (dol), calcite (cal) and tremolite (tre) in a thin section; plane polarized light (top) and crossed polars (bottom).

Table 1. Chemical composition of yangzhumingite.

Constituent	wt%	Range	SD	Probe standard
SiO_2	58.8	56.43–60.99	1.36	Wollastonite
Al_2O_3	0.41	0.03–1.49	0.42	Sillimanite
MgO	24.7	24.41–25.64	0.34	Mg_2SiO_4
FeO	1.00	0.34–2.05	0.41	Fe_2SiO_4
MnO	0.02	0.00–0.05	0.02	Rhodonite
TiO_2	0.01	0.00–0.06	0.01	Anatase
K_2O	8.20	7.73–8.81	0.33	K-feldspar
Li_2O^a	1.10			Zinnwaldite
Na_2O	0.06	0.03–0.11	0.02	Albite
CaO	0.04	0.01–0.09	0.02	Wollastonite
BaO	0.03	0.00–0.15	0.04	Barite
F	9.04	7.04–10.59	0.84	CaF_2
H_2O^b	0.17			
O=F	−3.81			
Total	99.75			

5. Crystallography

Single-crystal X-ray studies could not be carried out. The fragments picked out from the thin section used for the chemical analysis were curved and cleaved too finely for single-crystal XRD measurement. X-ray powder-diffraction data were collected using a 114.6 mm diameter Gandolfi camera (Ni-filtered Cu$K\alpha$ radiation). Data were recorded on an imaging plate (IP), processed with a Fuji BAS-2500 bio-image analyzer using a computer program written by Nakamuta (1999), and indexed by analogy with those of synthetic $KMg_{2.5}Si_4O_{10}F_2$ (Toraya *et al.*, 1976). The unit-cell parameters were refined from the powder XRD data using the computer program of Toraya (1993). X-ray powder diffraction data are given in Table 2. Yangzhumingite is monoclinic, space group $C2/m$, with unit-cell parameters $a = 5.249(4)$, $b = 9.095(5)$, $c = 10.142(5)$ Å, $\beta = 99.96(6)°$, $V = 476.9(5)$ Å^3, $Z = 2$. The a:b:c ratio calculated from the unit-cell parameters is 0.577:1:1.115.

Table 2. Powder X-ray diffraction data for yangzhumingite. Minor unindexed peaks are attributed to the presence of admixed richterite.

Yangzhumingite						Richterite, Ca-rich, syn.[a]				
I	$d_{meas.}$	$d_{calc.}$	h	k	l	I	d	h	k	l
95	**10.03**	**9.99**	**0**	**0**	**1**					
7	8.48					45	8.48	1	1	0
12	5.01	4.99	0	0	2	4	5.09	0	0	1
3	4.88					14	4.80	2	0	0
45	**4.51**	4.55	0	2	0					
		4.49	1	1	0	18	4.50	0	4	0
15	4.36	4.35	1	1	$\bar{1}$					
12	3.89	3.89	1	1	1					
38	3.63	3.62	1	1	$\bar{2}$					
48	**3.37**	3.36	0	2	2	25	3.39	1	3	1
		3.33	0	0	3					
10	3.29					50	3.28	$\bar{2}$	4	0
41	**3.12**	3.12	1	1	2	100	3.15	3	1	0
9	2.95					12	2.953	2	2	1
49	**2.90**	2.89	1	1	$\bar{3}$					
4	2.83					20	2.821	3	3	0
5	2.75					6	2.733	$\bar{3}$	3	1
16	2.71	2.69	0	2	3	14	2.707	1	5	1
		2.62	1	3	0					
43	**2.62**	2.61	2	0	$\bar{1}$					
67	**2.59**	**2.59**	**1**	**3**	$\bar{1}$					
		2.58	**2**	**0**	**0**	6	2.585	0	6	1
9	2.54	2.50	1	1	3					
		2.50	0	0	4					
14	2.48	2.48	1	3	1					
		2.48	2	0	$\bar{2}$					
100	**2.41**	**2.40**	**1**	**3**	$\bar{2}$					
		2.40	**2**	**0**	**1**					
14	2.35	2.34	1	1	$\bar{4}$	8	2.334	$\bar{3}$	5	1
		2.27	0	4	0					
12	2.27	2.27	2	2	$\bar{1}$					
7	2.25	2.25	2	2	0					
6	2.22	2.22	0	4	1					
40	2.15	2.15	1	3	$\bar{3}$	8	2.165	1	3	2
		2.15	2	0	2					
5	2.13	2.13	2	2	1					
6	2.05	2.07	0	4	2					
		2.06	1	1	4					
7	2.02	2.01	2	2	$\bar{3}$					
5	2.00	2.00	0	0	5					
		1.975	2	0	$\bar{4}$					
12	1.974	1.974	1	3	3					
		1.891	1	3	$\bar{4}$					
3	1.889	1.890	2	0	3					
		1.878	0	4	3					
4	1.808	1.811	2	2	$\bar{4}$					
3	1.794									

Table 2. Continued.

Yangzhumingite					
I	$d_{meas.}$	$d_{calc.}$	h	k	l
5	1.713	1.716	1	5	0
		1.716	2	4	$\bar{1}$
5	1.677	1.681	0	4	4
		1.675	1	5	1
		1.675	2	4	$\bar{2}$
30	1.657	1.659	1	3	$\bar{5}$
		1.658	2	0	4
		1.625	3	1	$\bar{3}$
7	1.623	1.624	3	1	1
7	1.593	1.595	2	4	$\bar{3}$
		1.595	1	5	2
		1.562	1	5	$\bar{3}$
7	1.560	1.562	2	4	2
		1.525	2	0	$\bar{6}$
15	1.523	1.525	1	3	5
		1.516	0	6	0
36	1.514	1.515	3	3	$\bar{1}$
		1.499	0	6	1
		1.498	3	3	$\bar{2}$
13	1.497	1.498	3	3	0
4	1.461	1.464	1	3	$\bar{6}$
		1.463	2	0	5
7	1.446	1.446	2	2	$\bar{6}$
		1.352	2	0	$\bar{7}$
12	1.351	1.352	1	3	6
15	1.307	1.308	2	6	0
		1.307	4	0	$\bar{2}$
		1.296	2	2	$\bar{7}$
		1.296	0	6	4
		1.296	3	3	$\bar{5}$
11	1.294	1.295	3	3	3
		1.282	2	6	1
8	1.280	1.282	4	0	$\bar{3}$
5	1.253	1.255	2	6	$\bar{3}$
		1.251	2	2	6
6	1.207	1.210	1	7	2
		1.209	4	2	1
		1.209	0	4	7
5	1.118	1.119	4	0	$\bar{6}$
		1.119	2	6	4

[a]ICDD PDF# 31-1284.

6. Discussion

Yangzhumingite is a member of the mica group (Strunz and Nickel class 9.EC.10: Strunz & Nickel, 2001) and, through its tetrasilicic, fluorine-dominant and interlayer K-dominant character, it represents the Mg-analogue of montdorite, $(K, Na)(Fe^{2+},Mn^{2+},Mg)_{2.5}Si_4O_{10}[F,(OH)]_2$. The crystal structure of synthetic $KMg_{2.5}Si_4O_{10}F_2$ was determined by Toraya *et al.* (1976). The synthetic equivalent of yangzhumingite is a white powder and is used in paint compounding agents and lubricants (*e.g.*, Topy Industry Limited, PDM-K(G)325).

The length of the *b*-axis is closely related to the size of the octahedral sites in micas. The *d*-spacing of 060 reflection in the XRD pattern, d_{060}, has been used as a preliminary indicator to distinguish di-octahedral and tri-octahedral micas from each other (Brown & Brindley, 1980). Muscovite and celadonite, di-octahedral micas, show a smaller d_{060} (*ca.* 1.50 Å) than the tri-octahedral micas phlogopite and annite, (*ca.* 1.53–1.56 Å) (Table 3). The approximate mean interatomic distances for Mg- and Fe^{2+}-O at the octahedral sites in tri-octahedral micas are 2.07 and 2.12 Å, respectively, and are comparable to the sums of the effective ionic radii of cations (Shannon, 1976) and O^{2-} anion. Those are shorter for trivalent cations in di-octahedral micas, such as Al^{3+} and Fe^{3+} (*ca.*, 1.94 and 2.04 Å for Al-O and Fe-O, respectively, see Table 3). These interatomic distances are short enough to reduce the d_{060}, even though the mean □-O distances, the octahedral distance from the center of the vacant site to the nearest six oxygen atoms in the di-octahedral micas, are not less than the Mg- and Fe^{2+}-O distances. In yangzhumingite the d_{060} value (1.516 Å) and the length of the *b*-parameter (9.095 Å) are intermediate between those of the di- and tri-octahedral micas. The length of the *b*-parameter of yangzhumingite is comparable to those of $KMg_{2.5}Si_4O_{10}F_2$ (Toraya *et al.*, 1976), the synthetic equivalent of yangzhumingite, and its OH-analogue $[KMg_{2.5}Si_4O_{10}(OH)_2]$ (Seifert & Schreyer, 1971).

The structural position of Li, the minor constituent, in yangzhumingite is an interesting subject from viewpoint of crystal chemistry. The univalent Li^+ usually occupies the octahedral sites in mica-group minerals. An empirical formula with Li^+ at the octahedral sites could indeed be expressed as $(K_{0.70}Na_{0.01})(Mg_{2.48}Li_{0.30}Fe_{0.06})(Si_{3.96}Al_{0.03})O_{10}[F_{1.92}(OH)_{0.08}]$ for yangzhumingite with the present chemical data, leading to a simplified formula $(K,\square)(Mg,Li,\square)_3Si_4O_{10}(F,OH)_2$, with vacancies, "□", at both the octahedral and interlayer cation sites. This cation distribution suggests a solid solution towards $K(Mg_2Li)Si_4O_{10}F_2$ [tainiolite] and a virtual talc-like end-member, $\square Mg_3Si_4O_{10}F_2$ from the ideal composition of yangzhumingite, $KMg_{2.5}Si_4O_{10}F_2$.

The crystal structure of Li-bearing micas was determined and refined for polylithionite (Brigatti *et al.*, 2000, 2005), trilithionite (Brigatti *et al.*, 2007), masutomilite (Mizota *et al.*, 1986; Brigatti *et al.*, 2007), and norrishite (Tyrna & Guggenheim, 1991). In the crystal structure of these tri-octahedral micas, the octahedral Li-O distances vary between 2.12 and 2.15 Å. These distances are comparable to the sum of ionic radii of Li^+ and O^{2-} (0.76 and 1.40 Å, respectively; Shannon, 1976), and are longer than the usual Mg-O distances, *ca.* 2.06 Å.

Since the ionic radius of Li^+ (0.76 Å, Shannon, 1976) is slightly larger than Mg^{2+} (0.72 Å, Shannon, 1976), the introduction of Li^+ into the octahedral site(s) for Mg^{2+} should not induce a shortening of the M_{oct}-O distance, and consequently should keep or increase the length of the *b*-axis and, d_{060}. However, the *b*-parameter of yangzhumingite (9.095 Å) is shorter than those of fluorophlogopite (9.189 Å; Gianfagna *et al.*, 2007) and phlogopite (9.2036 Å; Redhammer & Roth, 2002). Nonetheless, the replacement of smaller Si^{4+} for larger Al^{3+} at the tetrahedral sheet can decrease the lateral dimension to reduce the tetrahedral

Table 3. A comparison of lattice parameters, 060 *d*-spacing and mean octahedral interatomic distances.

Mineral name	Formula	*a* (Å)	*b* (Å)	*c* (Å)	β (°)	*V* (Å^3)	d_{060} (Å)	M_{octa}-O distances(Å) and occupants			
Yangzhumingite[a]	$KMg_{2.5}Si_4O_{10}F_2$	5.249(4)	9.095(5)	10.142(5)	99.96(6)	476.9(5)	1.516				
Synthetic[b]	$KMg_{2.5}Si_4O_{10}F_2$	5.253(1)	9.086(2)	10.159(1)	99.89(3)	477.7	1.514	2.062	Mg,□	2.064	Mg,□
Synthetic[c]	$KMg_{2.5}Si_4O_{10}(OH)_2$	5.256[5]	9.089[8]	10.201[10]	99.98[9]	479.9	1.515				
Montdorite[d]	$KFe^{2+}{}_{1.5}Mn^{2+}{}_{0.5}Mg_{0.5}Si_4O_{10}F_2$	5.310(6)	9.20(1)	10.175(5)	99.9(1)	489.67	1.533				
Muscovite[e]	$KAl_2(AlSi_3)O_{10}(OH)_2$	5.199(2)	9.0266(19)	20.106(4)	95.78(4)	938.7(5)	1.504	2.253	□	1.94	Al
Muscovite[f]	$KAl_2(AlSi_3)O_{10}(OH)_2$	5.180(4)	8.993(6)	20.069(13)	95.69(8)	930(1)	1.499			1.924	Al
Muscovite[g]	$KAl_2(AlSi_3)O_{10}(OH)_2$	5.197(1)	9.019(2)	20.068(3)	95.71(1)	936	1.503	2.219	□	1.937	Al,Fe^{2+},Li
Aluminoceladonite[h]	$KAl^{3+}(Mg,Fe^{2+})Si_4O_{10}(OH)_2$	5.2227(3)	9.0195(3)	10.0767(8)	100.82(1)	466.2	1.503	2.171	□	1.999	Al,Mg
Celadonite[h]	$KFe^{3+}(Mg,Fe^{2+})Si_4O_{10}(OH)_2$	5.2291(5)	9.051(1)	10.144(4)	100.59(2)	471.9	1.509	2.132	□	2.047	Fe^{3+},Mg
Paragonite[i]	$NaAl_2(AlSi_3)O_{10}(OH)_2$	5.140(2)	8.911(5)	19.380(12)	94.62(1)	884.8(1)	1.485				
Phlogopite[j]	$KMg_3AlSi_3O_{10}(OH)_2$	5.330(1)	9.239(1)	10.305(1)	99.89(1)	499.9	1.54	2.084	Mg,Fe	2.081	Mg,Fe
Phlogopite[k]	$KMg_3AlSi_3O_{10}(OH)_2$	5.3252(2)	9.2205(3)	10.2458(4)	99.994(3)	495.442	1.537	2.079	Mg,Fe	2.072	Mg,Fe
Phlogopite[l]	$KMg_3AlSi_3O_{10}(OH)_2$	5.343(1)	9.247(2)	10.397(3)	100.04(2)	505.8(2)	1.541	2.092	Mg,Fe^{2+},Li	2.064	Mg,Fe^{2+},Al
Phlogopite[m]	$KMg_3AlSi_3O_{10}(OH)_2$	5.310(1)	9.193(2)	10.096(4)	100.00(3)	485.36(24)	1.532	2.067	Mg,Fe^{3+}	2.06	Mg,Fe^{2+}
Phlogopite[n]	$KMg_3AlSi_3O_{10}(OH)_2$	5.305(2)	9.199(2)	10.232(4)	100.03(2)	491.7(4)	1.533	2.077	Mg,Li,Fe	2.078	Mg,Li,Fe
Phlogopite[o]	$KMg_3AlSi_3O_{10}(OH)_2$	5.346(1)	9.258(2)	10.208(2)	100.12(1)	497.37	1.543	2.086	Fe,Mg,Li	2.074	Mg,Fe
Synthetic[p]	$KMg_3AlSi_3O_{10}(OH)_2$	5.3158(24)	9.2036(34)	10.3100(57)	99.891(59)	496.91	1.534	2.074	Mg	2.072	Mg
Fluorophlogopite[q]	$KMg_3AlSi_3O_{10}F_2$	5.3094(4)	9.1933(7)	10.1437(8)	100.062(5)	487.51(7)	1.532	2.064	Mg	2.061	Mg,Fe
Synthetic[q]	$KMg_3AlSi_3O_{10}F_2$	5.3167(2)	9.2123(3)	10.1534(3)	100.105(2)	489.59	1.535	2.064	Mg	2.063	Mg
Aspidolite[r]	$NaMg_3AlSi_3O_{10}(OH)_2$	5.291(8)	9.16(2)	10.12(2)	105.1(1)	473(1)	1.527				
Synthetic[p]	$KFe_3AlSi_3O_{10}(OH)_2$	5.4059(21)	9.3639(27)	10.3235(41)	100.200(46)	514.32	1.561	2.124	Fe^{2+}	2.119	Fe^{2+}
Polylithionite[s]	$KLi_2AlSi_4O_{10}F_2$	5.262(1)	9.085(2)	10.099(2)	100.72(1)	474.4	1.514	2.124	Li,Fe	2.122	Li,Fe
										1.885	Al,Li
Polylithionite[t]	$KLi_2AlSi_4O_{10}F_2$	9.029(4)	5.203(1)	20.201(6)	99.35(3)	936.4(4)		2.122	Li	1.975	Al.Li
Trilithionite[u]	$KLi_{1.5}Al_{1.5}AlSi_3O_{10}F_2$	5.264(1)	9.086(2)	10.099(3)	100.719(5)	474.6(2)	1.514	1.883	Al	2.131	Li,Fe
										2.123	Li,Fe
Synthetic[v]	$KLiMg_2Si_4O_{10}F_2$	5.231(1)	9.065(2)	10.140(1)	99.86(2)	473.8(1)	1.511	2.058	Mg,Li	2.061	Mg,Li
Shirokshinite[w]	$KNaMg_2Si_4O_{10}F_2$	5.269(2)	9.092(11)	10.197(3)	100.12(7)	480.9(4)	1.515	2.11	Na	2.081	Mg
Masutomilite[x]	$KLiAlMn^{2+}AlSi_3O_{10}F_2$	5.262(2)	9.102(3)	10.094(3)	100.83(2)		1.517	1.89		2.12	
Masutomilite[u]	$KLiAlMn^{2+}AlSi_3O_{10}F_2$	5.2984(3)	9.1461(6)	10.0966(37	100.818(4)	480.58(5)	1.524	1.883	Al	2.131	Mn,Li
										2.137	Mn,Li
Norrishite[y]	$KLiMn^{3+}{}_2Si_4O_{12}$	5.289(3)	8.914(3)	10.62(7)	98.22(5)		1.486	2.121	Li	2.037	Mn

[a]Present study; [b]Toraya *et al.* (1976); [c]Seifert & Schreyer (1971); [d]Robert & Maury (1979); [e]Richardson & Richardson (1982); [f]Liang & Hawthorne (1996); [g]Brigatti *et al.* (2001a); [h]Drits *et al.* (2010); [i]Comodi & Zanazzi (2000); [j]Brigatti *et al.* (2001b); [k]Matarrese *et al.* (2008); [l]Hawthorne *et al.* (1999); [m]Mesto *et al.* (2006); [n]Ferraris *et al.* (2001); [o]Schingaro *et al.* (2001); [p]Redhammer & Roth (2002); [q]Gianfagna *et al.* (2007); [r]Banno *et al.* (2005); [s]Brigatti *et al.* (2000); [t]Brigatti *et al.* (2005); [u]Brigatti *et al.* (2007); [v]Toraya *et al.* (1977); [w]Pekov *et al.* (2003); [x]Mizota *et al.* (1986); [y]Tyrna & Guggenheim (1991).

rotation. This shrinkage is adverse for the introduction of larger Li^+ ion into the Mg^{2+} octahedra, which enlarges the misfit between tetrahedral and octahedral sheets. Thus, with the length of the *b*-parameter, it is speculated that, in yangzhumingite, Li^+ ions do not occupy the octahedral site, but rather replace the interlayer K^+. The structure model with Li^+ in interlayer suggests a solid solution between the ideal formula of yangzhumingite [$KMg_{2.5}Si_4O_{10}F_2$] and a hypothetical $LiMg_{2.5}Si_4O_{10}F_2$. A smaller Li^+ can substitute a part of larger K^+ in a cavity of tight framework, whereas the larger cation can not replace the smaller cation without effect on the framework. The minor (0.3 *apfu*) Li^+ seems to stay in a large interlayer space, which is borne by the major (0.7 *apfu*) K^+ at the neighboring interlayer cation sites in the crystal structure of yangzhumingite.

Toraya *et al.* (1977) reported the crystal structure of $K(Mg_2Li)Si_4O_{10}F_2$, the synthetic equivalent of tainiolite. Their analysis showed that Li^+ does not preferentially occupy one of octahedral sites, but distributes with Mg^{2+} into all of the octahedral sites, and gave the mean (Mg,Li)-O distances of 2.058 and 2.061 Å. These (Mg,Li)-O distances indicate no enlargement of the usual Mg-O distances (*ca.* 2.06 Å) by the substitution of Li^+ for Mg^{2+} in the mica structure. However, Toraya *et al.* (1977) gave no chemical data for their synthesized crystal to confirm the Li^+ in the crystal.

A refinement of occupancy factors of Li at the octahedral and interlayer cation sites could help to study the speciation of Li in yangzhumingite. As discussed above, so far we were not able to obtain single-crystal diffraction data because of the small size of the curved or cleaved single crystals. The measured powder XRD pattern of yangzhumingite showed no any remarkable and alternative identity to a specific pattern among the simulated XRD patterns with different distributions of Li^+ in the interlayer cation site or octahedral sites.

Phlogopite associated with yangzhumingite showed replacement of (OH) with F, with the F/[F + (OH)] ratios ranging between 0.25 and 0.38 (Shimazaki *et al.*, 2008b). The geneses of yangzhumingite, fluorotetraferriphlogopite and the F-bearing phlogopite, as well as the other associated minerals such as fluorbritholite-(Ce), huanghoite-(Ce), and bastnäsite-(Ce), can be correlated with a F-rich geochemical environment in Bayan Obo.

Acknowledgements: The authors wish to thank Mr. Zhang Guozhong and the staff of Baotou Iron & Steel Group for their cooperation. We express our appreciation to Mr. Shun-ichi Ohta of TOPY Industries, Limited for his donation of the synthetic $KMg_{2.5}Si_4O_{10}F_2$ crystals and with technical information. Special thanks are extended to Prof. Peishan Zhang and Prof. Shoji Higashi for their important suggestion on the geochemistry and crystallography. Prof. Luca Bindi, the Associate Editor, Prof. Emanuela Schingaro and Prof. Frederic Hatert, the referees, are thanked for their helpful reviews.

References

Banno, Y., Miyawaki, R., Kogure, T., Matsubara, S., Kamiya, T., Yamada, S. (2005): Aspidolite, the Na analogue of phlogopite, from Kasuga-mura, Gifu Prefecture, central Japan: description and structural data. *Mineral. Mag.*, **69**, 1047–1057.

Brigatti, M.F., Lugli, C., Poppi, L., Foord, E.E., Kile, D.E. (2000): Crystal chemical variations in Li- and Fe-rich micas from Pikes Peak batholith (central Colorado). *Am. Mineral.*, **85**, 1275–1286.

Brigatti, M.F., Kile, D.E., Poppi, M. (2001a): Crystal structure and crystal chemistry of lithium-bearing muscovite-2M_1. *Can. Mineral.*, **39**, 1171–1180.

Brigatti, M.F., Medici, L., Poppi, L., Vaccaro, C. (2001b): Crystal chemistry of trioctahedral micas-1*M* from the Alto Paranaíba Igneous Province, southeastern Brazil. *Can. Mineral.*, **39**, 1333–1345.

Brigatti, M.F., Caprilli, E., Malferrari, D., Medici, L., Poppi, L. (2005): Crystal structure and chemistry of trilithionite-2M_2 and polylithionite-2M_2. *Eur. J. Mineral.*, **17**, 475–481.

Brigatti, M.F., Mottana, A., Malferrari, D., Cibin, G. (2007): Crystal structure and chemical composition of Li-, Fe-, and Mn-rich micas. *Am. Mineral.*, **92**, 1395–1400.

Brown, G., Brindley, G.W. (1980): X-ray diffraction procedure for clay mineral identification. *in* ''Crystal structures of clay minerals and their X-ray identification'', G.W. Brindley & G. Brown, eds. Mineralogical Society, London, 305–360.

Comodi, P. & Zanazzi, P.F. (2000): Structural thermal behavior of paragonite and its dehydroxylate: a high-temperature single-crystal study. *Phys. Chem. Miner.*, **27**, 377–385.

Drits, V.A., Zviagina, B.B., McCarty, D.K., Salyn, A.L. (2010): Factors responsible for crystal-chemical variations in the solid solutions from illite to aluminoceladonite and from glauconite to celadonite. *Am. Mineral.*, **95**, 348–361.

Ferraris, G., Gula, A., Ivaldi, G., Nespolo, M., Sokolova, E., Uvarova, Y., Khomyakov, A.P. (2001): First structure determination of an MDO-2*O* mica polytype associated with a 1*M* polytype. *Eur. J. Mineral.*, **13**, 1013–1023.

Gianfagna, A., Scordari, F., Mazziotti-Tagliani, S., Ventruti, G., Ottolini, L. (2007): Fluorophlogopite from Biancavilla (Mt. Etna, Sicily, Italy): crystal structure and crystal chemistry of a new F-dominant analog of phlogopite. *Am. Mineral.*, **92**, 1601–1609.

Hawthorne, F.C., Teertstra, D.K., Černý, P. (1999): Crystal-structure refinement of a rubidian cesian phlogopite. *Am. Mineral.*, **84**, 778–781.

Liang, J.-J., Hawthorne, F.C. (1996): Rietveld refinement of micaceous materials: muscovite-2M_1, a comparison with single-crystal structure refinement. *Can. Mineral.*, **34**, 115–122.

Matarrese, S., Schingaro, E., Scordari, F., Stoppa, F., Rosatelli, G., Pedrazzi, G., Ottolini, L. (2008): Crystal chemistry of phlogopite from Vulture-S. Michele Subsynthem volcanic rocks (Mt. Vulture, Italy) and volcanological implications. *Am. Mineral.*, **93**, 426–437.

Mesto, E., Schingaro, E., Scordari, F., Ottolini, L. (2006): An electron microprobe analysis, secondary ion mass spectrometry and single crystal X-ray diffraction study of phlogopites from Mt. Vulture, Potenza, Italy: consideration of cation partitioning. *Am. Mineral.*, **91**, 182–190.

Miyawaki, R., Shimazaki, H., Shigeoka, M., Yokoyama, K., Matsubara, S., Yurimoto, H., Yang, Z., Zhang, P. (2011):

Fluorokinoshitalite and fluorotetraferriphlogopite: new species of fluoro-mica from Bayan Obo, Inner Mongolia, China. *Clay Sci.*, **15**, in press.

Mizota, T., Kato, T., Harada, K. (1986): The crystal structure of masutomilite, Mn analogue of zinnwaldite. *Mineral. J.*, **13**, 13–21.

Nakamuta, Y. (1999): Precise analysis of a very small mineral by an X-ray diffraction method. *J. Mineral. Soc. Jpn.*, **28**, 117–121 (in Japanese with English abstract).

Pekov, I.V., Chukanov, N.V., Ferraris, G., Ivaldi, G., Pushcharovsky, D.Yu., Zadov, A.E. (2003): Shirokshinite, $K(NaMg_2)Si_4O_{10}F_2$, a new mica with octahedral Na from Khibiny massif, Kola Peninsula: descriptive data and structural disorder. *Eur. J. Mineral.*, **15**, 447–454.

Redhammer, G.J., Roth, G. (2002): Single-crystal structure refinements and crystal chemistry of synthetic trioctahedral micas $KM_3(Al^{3+},Si^{4+})_4O_{10}(OH)_2$, where $M = Ni^{2+}$, Mg^{2+}, Co^{2+}, Fe^{2+}, or Al^{3+}. *Am. Mineral.*, **87**, 1464–1476.

Richardson, S.M., Richardson, J.W., Jr. (1982): Crystal structure of a pink muscovite from Archer's Post, Kenya: implications for reverse pleochroism in dioctahedral micas. *Am. Mineral.*, **67**, 69–75.

Robert, J.-L., Maury, R.C. (1979): Natural occurrence of a (Fe,Mn,Mg) tetrasilicic potassium mica. *Contrib. Mineral. Petrol.*, **68**, 117–123.

Schingaro, E., Scordari, F., Ventruti, G. (2001): Trioctahedral micas-1*M* from Mt. Vulture (Italy): structural disorder and crystal chemistry. *Eur. J. Mineral.*, **13**, 1057–1069.

Seifert, F., Schreyer, W. (1971): Synthesis and stability of micas in the system K_2O–MgO–SiO_2–H_2O and their relations to phlogopite. *Contrib. Mineral. Petrol.*, **30**, 196–215.

Shannon, R.D. (1976): Revised effective ionic radii and systematic studies of interatomic distances in halides and chalcogenides. *Acta Crystallogr.*, **A32**, 751–767.

Shimazaki, H., Miyawaki, R., Yokoyama, K., Matsubara, S., Yang, Z. (2008a): Zhangpeishanite, BaFCl, a new mineral in fluorite from Bayan Obo, Inner Mongolia, China. *Eur. J. Mineral.*, **20**, 1141–1144.

Shimazaki, H., Miyawaki, R., Yokoyama, K., Matsubara, S., Yang, Z., Shigeoka, M. (2008b): A reconnaissance study on minerals from the Bayan Obo Nb-REE-Fe deposit, Inner Mongolia, China. *Bull. Natl. Mus. Nat. Sci., Ser. C*, **34**, 1–26.

Strunz, H. & Nickel, E.H. (2001): Strunz mineralogical tables. Chemical-structural mineral classification system. 9th Edition, E. Schweizerbart'sche Verlagsbuchhandlung (Nägele u. Obermiller), Stuttgart, 663–669.

Toraya, H. (1993): The determination of unit-cell parameters from Bragg reflection data using a standard reference material but without a calibration curve. *J. Appl. Crystallogr.*, **26**, 583–590.

Toraya, H., Marumo, F., Daimon, M., Kondo, R. (1976): The crystal structure of tetrasilicic potassium fluor mica, $KMg_{2.5}Si_4O_{10}F_2$. *Z. Kristallogr.*, **144**, 42–52.

Toraya, H., Iwai, S., Marumo, F., Hirao, M. (1977): The crystal structure of taeniolite, $KLiMg_2Si_4O_{10}F_2$. *Z. Kristallogr.*, **146**, 73–83.

Tyrna, P.L. & Guggenheim, S. (1991): The crystal structure of norrishite, $KLiMn^{3+}{}_2Si_4O_{12}$: an oxygen-rich mica. *Am. Mineral.*, **76**, 266–271.

Yurimoto, H., Yamashita, A., Nishida, N., Sueno, S. (1989): Quantitative SIMS analysis of GSJ rock reference samples. *Geochem. J.*, **23**, 215–236.

Zhang, P. & Tao, K. (1986): Bayan Obo mineralogy, Science Press, Beijing, China, 208 p. (in Chinese with an English comprehensive synopsis).

Received 19 November 2010
Modified version received 18 January 2011
Accepted 24 February 2011